Dynamic Mechanical and Vibration Damping Properties of Polyurethane Compositions

DENNIS T. H. WONG* and H. LEVERNE WILLIAMS, *Department of Chemical Engineering and Applied Chemistry, University of Toronto, Toronto, Ontario M5S 1A4, Canada*

Synopsis

A series of polyurethane compositions with varying comonomer ratio and structure, polyblends with epoxy resin, and filled systems with mica and calcium carbonate were prepared. The dynamic mechanical properties of the compositions were measured at 110 Hz using a Rheovibron. The vibration damping properties were measured using a Brüel and Kjaer damping modulus apparatus with steel strips as substrate, the polyurethane compositions as coatings, and, when used, a constraining layer of aluminum or epoxy. The damping curves by the two techniques were similar in shape. Furthermore, the damping properties of the compositions in both extensional and constrained layer configurations could be estimated from the dynamic mechanical properties. The width of the damping region in terms of the temperature range was used as a criterion for effectiveness. Very wide ranges of temperature, and hence frequency, fell within the damping region which was broadened to as much as −40–60°C by the use of bulky backbone chain polymers, by polyblending with epoxy, and by filling with mica. Mica in an extensional mode configuration could be considered as equivalent to a constraining layer for purposes of calculation. The data agree well with the general view that extensional mode damping requires a high loss modulus and constrained mode damping a high loss factor, in both cases being more effective if the storage modulus were also high.

INTRODUCTION

Damping of vibrations is required for many purposes, but in particular to reduce noise levels in the workplace. Of the many sources of noise, one is resonating panels or structural members which rattle or drum in response to some source of mechanical energy. A typical example would be a deck or door panel of an automobile. Early in the automobile industry the utility of a mastic deadener composed of asphalt filled with inorganic filler or fibers was recognized.[1] Soon viscoelastic damping materials appeared.[2] Oberst[3] studied extensional type damping composites composed of a viscoelastic layer on an elastic substrate (steel). He showed that the composite loss factor depended on the loss modulus of the viscoelastic layer. The principles were developed further by Ross, Ungar, and Kerwin.[4] The composite damping factor was related to the loss modulus of the viscoelastic layer divided by the elastic modulus of the substrate[3] and to the square of the thickness ratio.[4] These damping agents are easy to apply by trowel, brush, or spray. Ball and Salyer[5] described typical systems and the data obtained.

The constrained layer configuration yielded better damping.[3] This sandwich structure is composed of the substrate, a viscoelastic layer, and a second stiff

* Present address: Shaw Pipe Protection Ltd., Toronto, Canada.

Journal of Applied Polymer Science, Vol. 28, 2187–2207 (1983)
 CCC 0021-8995/83/072187-21$03.10

elastic layer which may be metallic or plastic. Oberst outlined the basic principles related to thickness ratios. The theory was advanced by Kerwin[6] and Ungar.[7] It was noted in particular that the composite damping factor was related to the loss factor of the viscoelastic layer.[4,7] Yin et al.[8] and Preiss et al.[9] applied the principles to other than simple plates and verified the concepts.

The suitability of polyurethanes for the viscoelastic damping layer was suggested by Lewis and Elder,[10] and Yin[11] outlined some of the guidelines for choice of chemical composition. Many investigations on the morphology, mechanical properties, and transitional behavior of polyurethanes have been published, including polyblends, interpenetrating networks, and graft and block copolymers which include polyurethane portions.

Included have been studies of plasticizers and fillers in the viscoelastic layer. In general, comparison of the damping data and the dynamic mechanical properties showed that materials with a high loss modulus coupled with a high dynamic or storage modulus were most effective. Extensional damping correlated with the loss modulus while constrained layer damping correlated with the loss factor of the viscoelastic layer.

Chen undertook a broad study of relatively high modulus viscoelastic polyurethane, polyester, or epoxy resins, which were flexibilized with elastomeric polymers in sound absorption[12] and vibration damping[13] studies. He utilized foamed polyurethane compositions preferably but not exclusively. The dynamic mechanical properties of the styrene-crosslinked polyester used by Chen were measured before and after blending with poly(methyl methacrylate) powder, lead powder, plasticized poly(vinyl chloride)/butadiene–acrylonitrile elastomer blend, and styrene–butadiene copolymer (70/30). Whereas the solid fillers affected the width and position of the tan δ peak very little, the incorporation of the elastomers broadened the peaks and shifted them to encompass room temperature in agreement with the damping performance observed separately. Subsequently,[14] the study turned to elastomeric polyurethanes containing fillers to raise the modulus. Whereas polypropylene powder was ineffective, both mica and calcium carbonate broadened the tan δ peak and increased the value of tan δ above the peak temperature to encompass a broad temperature range over which the viscoelastic polymer might be expected to be useful for vibration damping uses. The present study is a continuation of these studies with emphasis on unfoamed polymers in both the extensional and constrained layer configurations.

MATERIALS AND PROCEDURES

Multrathane F242, isocyanate-terminated short chain poly(ethylene adipate) equivalent weight 900, Multrathane R144 hydroxy-terminated poly(butylene adipate) equivalent weight 1000, Multrathane F222 hydroxy-terminated poly(ethylene/butylene adipate) copolymer equivalent weight 1000, Multrathane XA 1,4-di(ethoxy-β-hydroxy)benzene from Mobay Chemical Corp., Toronto, Ontario.

TDI, toluene-2,4-diisocyanate, Dupont Canada, Kingston, Ontario.

MDI, 4,4′-diphenylmethane diisocyanate, 1,4-butandiol, 1,10-decandiol, 1,5-pentandiol, 1,4-cyclohexandiol, 4,8-bis(hydroxymethyl)tricyclo(5,2,1,$0^{2,6}$)-decane coded XB, from Eastman Kodak Co., Toronto, Ontario.

Poly(ethylene oxide)diol molecular weights 600, 1000, 1540, 4000 and poly-(propylene oxide)diol, molecular weights 1000, 2000, from Polysciences Inc., Markham, Ontario.

Epon 815 epoxy resin, diglycidyl ether of bisphenol acetone with 11% butyl glycidyl ether, and T-1 Epon Curing Agent, a polyamine, from Shell Chemicals, Toronto, Ontario.

Triethylamine and calcium carbonate precipitated chalk, −325 mesh, Fisher Chemicals, Toronto.

Polypropylene, Profax 6301, Hercules Inc., Montreal, Quebec.

Stannous octoate T-9 and dibutyl tin dilaurate T-12, M&T Chemicals, Toronto.

Steel strips, 24 gauge, Fembo Metal Products Ltd., Toronto, degreased with trichloroethylene, immersed in dilute nitric acid 1:10 for 20 min at 333 K, rinsed with distilled water, then acetone, dried, and stored in a desiccator until used.

Aluminum foil, Alcan Products, Montreal, Quebec.

Mica, phlogopite suzorite variety, −10 + 20, −40 + 70, −80 + 325, and −325 mesh, Marietta Resources International, Montreal, Quebec.

The preparation of polymers based on Multrathane F242 was accomplished in the melt. The prepolymer was heated to 353 K and degassed under 760 mm mercury vacuum. The degassed resin was put into a reaction kettle and heated to 373 K. The equivalent weight of the diol and stannous octoate (0.01% based on the prepolymer) was separately heated to 373 K and mixed with the prepolymer, the components mixed under vacuum for 2 min, and then cast in silicone molds to be cured in an oven at 373 K for 4 h. The compositions of the polymers are shown in Table I. The compositions are coded by letters and numbers in brackets and also by longer codes based on abbreviations which more directly indicate the components.

In all cases the stoichiometric ratio was unity. Thus the prepolymers were chain extended with little crosslinking. The molecular weights were high so that

TABLE I
Composition of Various Polyurethanes[a]

Sample code	Composition designation	Composition
A	F242–1,4	Multrathane F242–1,4-butanediol
B	F242–1,10	Multrathane F242–1,10-decanediol
C	F242–XA	Multrathane F242–Multrathane XA [1,4-di(ethoxy-β-hydroxy)-benzene]
D	F242–XB	Multrathane F242–4,8-bis(hydroxymethyl)tricyclo-(5,2,1,$0^{2,6}$)decane
E	F242–F222	Multrathane F242–Multrathane F222
F	F242–R144	Multrathane F242–Multrathane R144
G	F242–1,4cy	Multrathane F242–1,4-cyclohexanediol
C/F-75/25		F242–hydroxyl equivalent 75% XA + 25% R144
C/F-50/50		F242–hydroxyl equivalent 50% XA + 50% R144
C/F-25/75		F242–hydroxyl equivalent 25% XA + 75% R144
D/F-75/25		F242–hydroxyl equivalent 75% XB + 25% R144
D/F-50/50		F242–hydroxyl equivalent 50% XB + 50% R144
D/F-25/75		F242–hydroxyl equivalent 25% XB + 75% R144

[a] Stoichiometry of isocyanate to hydroxyl is unity.

variations would not affect the results since the glass transition temperature and the dynamic mechanical properties are little affected by molecular weight in the high molecular weight range. The average molecular weight, average block length, branching, and crosslink density were not measured.

When the polyether diols were used, the same process was suitable with a nitrogen atmosphere. First the diisocyanate prepolymer was made by adding the stoichiometric amount of MDI to the short chain diol at 343 K for 3 h with 0.1% dibutyl tin dilaurate based on the long chain diol. The long chain diol was heated to 343 K and mixed with the prepolymer; the mixture was poured into silicone molds and cured in an oven at 373 K for 4 h. For the higher molecular weight long chain diols a solution process was used. For example, 25 g of MDI in 100 mL of 1-methyl-pyrrolidone-2 was heated to 373 K, and 3.1 g of ethylene glycol and 0.2 g of dibutyl tin dilaurate in 100 mL of the same solvent added with vigorous stirring. After 2 h at 373 K, 200 g of poly(ethylene oxide), molecular weight 4000, in 200 mL of solvent was added and the reaction continued for three hours. The polymer was precipitated in a large volume of water, filtered, washed with ethanol, and dried at 323 K for 2 days.

The polyurethane–epoxy blends were prepared by mixing the two prepolymers at 353 K. The polyamine (T-1) was used to catalyze the epoxy cure. The same equipment was used without vacuum except for degassing the reactants at 353 K. The reactants were mixed for 30 s, and then poured into silicone molds to cure at 373 K for two days. Samples for studies of vibration damping were set aside to cure slowly at room temperature.

Filled samples were hot pressed into thin sheets which were stacked and cut to shape before final hot pressing. The filler content was verified by ashing at 773 K.

Samples for dynamic mechanical testing were hot pressed and cut to shape. The sample for vibration damping measurements were prepared by stacking shaped sheets on the steel substrate before hot pressing between aluminum plates. Thickness was controlled by spacers and excess material was trimmed off.

A Rheovibron model DDV-II direct reading viscoelastometer was used for measuring the dynamic mechanical properties at 110 Hz over the temperature range 173–423 K. The complex, storage and loss moduli were calculated and the tangent of the phase angle recorded. The error constants were determined in the usual way.

The internal damping and dynamic modulus of elasticity were measured with a Brüel and Kjaer Complex Modulus Apparatus Type 3930 in connection with a Brüel and Kjaer Heterodyne Analyzer Type 2010 and Level Recorder Type 2305. The samples were steel bars coated with the polymer, mounted vertically in the apparatus, and the damping modulus unit in turn placed in an environmental chamber which operated over the range 223–373 K. When no ferromagnetic material was used, a high-μ disc was attached at each end of the sample. Measurements were made at four to six successive resonance modes. The dynamic modulus E' can be calculated from the relationship

$$E' = 48\pi^2 2\rho(l^2 f_n/HK_n^2)^2$$

in which ρ is the density, l the length (m), f_n is the frequency at the nth resonance mode, H is the thickness of the sample bar in the plane of the vibration, and K_n

is defined by

$$K_n = (n - \tfrac{1}{2})\pi.$$

The damping factor was determined from the sharpness of the resonance curves

$$d = \Delta f_n / f_n$$

in which f_n is the undamped resonance frequency of resonance mode n and Δf_n is the band width 3 dB down from the resonance peak. This calculation is speeded by using a Brüel and Kjaer "Q-rule BM1001." This method is suitable for values of d between 0.6 and 0.001. Alternatively for low damping material the reverberation method was used in which t is the time for the vibration amplitude to decrease by 60 dB, i.e.,

$$d = 2.2/tf_n \quad \text{or} \quad D_t/27.3f_n$$

where D_t is the decay rate ($dB \cdot s^{-1}$).

In addition to the damping factor (d) the data are given in the form ($2C/C_0$), expressed as a percent, the percent critical damping, which is numerically equal to 50(d). In the extensional mode, the loss factor for the composite d_c is a function of the loss factor of the damping layer, the ratio of the storage modulus of the viscoelastic layer to that of the elastic layer, and the ratio of the thickness of the viscoelastic layer to the thickness of the elastic layer squared.[3,7] With the constrained layer configuration[6,7] a complex damping factor d_c can be calculated again using the loss factor of the viscoelastic layer, the ratios of the thicknesses of the layers, and the reciprocal of the storage modulus of the elastic substrate.

The thickness of the viscoelastic layer H_2 to the thickness of the substrate H_1 is defined as h_2. Likewise the thickness of the constraining layer H_3 to the thickness of the substrate H_1 is defined as h_3.

Thermomechanical properties were determined using a DuPont 990 Instrument with a differential scanning calorimeter (DSC) cell at a program rate of 10K/min.

Density was measured according to ASTM D792-66 (A-1 and A-2).

Isocyanate was determined by the dibutyl amine method.

RESULTS AND DISCUSSION

Polyurethanes

The prepolymer was Multrathane F242 which is isocyanate-terminated and has an equivalent weight of about 900. It was reacted with a series of diols with equivalent weights varying from 45 to 1000. The data are in Figure 1 for the tan δ measurements. As the equivalent weight of the diol increases the peak tan δ value is shifted to lower temperatures, from 269 K for 1,4-butandiol (A) to 258 K for Multrathane R144 (F). When ring structured diols are used, the bulkier the ring in the backbone, the higher the peak temperature at which the tan δ peak occurs. In general the more flexible the chain, the lower the transition temperature. It should be noted in particular that the phenylene ring (of C) and the tricyclodecanyl ring (of D) in the backbone of the chain result in higher tan

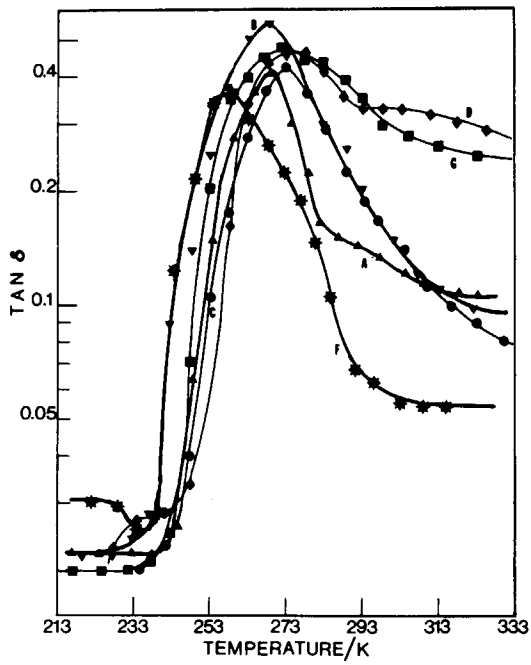

Fig. 1. Tan δ vs temperature for polyurethanes prepared from Multrathane F242 and: 1,4-butanediol (▲) (A); 1,10-decanediol (▼) (B); Multrathane R144 (✱) (F); 1,4-cyclohexanediol (■) (G); XB (♦) (D); and XA (●) (C); 110 Hz (see Table I for compositions).

δ values at temperatures above the peak temperature values, that is, a significant broadening of the peak in the higher temperature direction, presumably due to the stiffness and resultant viscosity increase at those temperatures.

The corresponding values for the loss and storage moduli were calculated. The storage moduli are very similar for all samples except that cured with Multrathane R144 (F). This long chain diol results in a lower E', and there is some indication that 1,4-butandiol (A) results in the highest. One might expect that the bulky ring diols incorporated into the backbone would result in a higher modulus, but in fact the results are lower, presumably because of a plasticizer-like effect since the concentrations are relatively low and the hard segment second phase is not expected to form as easily. The loss modulus data follow the corresponding tan δ values.

The effect of the bulky ring groups in the backbone chain was studied further by using mixtures with Multrathane R144 as shown in Table I, designated (C/F) and (D/F). The data in Figure 2 should be compared with those for Multrathane R144 alone (F) in Figure 1. In all cases the presence of the bulky backbone groups broadened the tan δ peak, the tricyclodecanyl ring (of D) being somewhat more effective than the phenylene ring (of C). The peak is broadened the most, by 10 K, when 50% of the hydroxy equivalent is in the form of the bulky backbone ring diol. This maximal broadening of the tan δ peak is observed, therefore, with only about 10% of the bulky backbone diol in the total blend. Both Multrathane F242 and R144 are long, linear, flexible units.

A study of the effect of soft segment length was undertaken with poly(ethylene

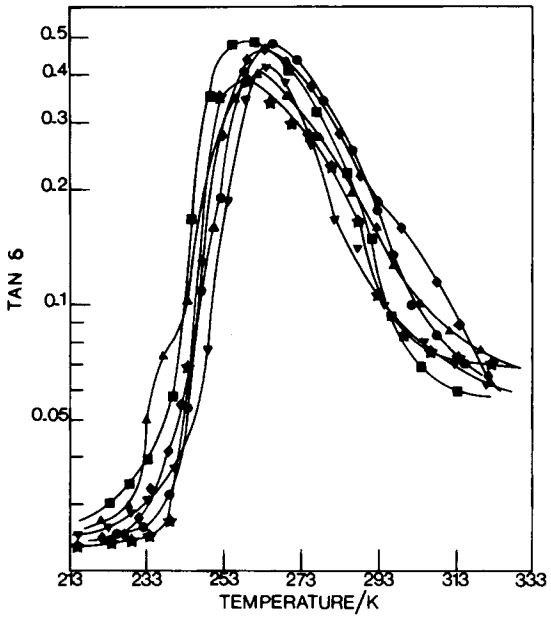

Fig. 2. Tan δ vs. temperature for polyurethanes prepared from Multrathane F242 and Multrathane R144 and XA (C/F) in the ratios 75/25 (▼), 50/50 (▲), and 25/75 equivalents (■), and Multrathane R144 and XB (D/F) in the ratios 75/25 (★), 50/50 (♦), and 25/75 equivalents (●); 110 Hz (see Table I for compositions).

oxide)diol and poly(propylene oxide)diol of various prepolymer chain lengths in combination with a hard segment from ethylene glycol and MDI. The solubility parameter of the latter is 21.8 $(J/cm^3)^{1/2}$ whereas that of the former is 19.4 and 18.9 $(J/cm^3)^{1/2}$, respectively. This difference in values suggests that the hard and soft segment domains might well separate and this should affect the dynamic mechanical properties.

Figure 3 shows the data obtained with the poly(ethylene oxide) diols. Below a molecular weight of 1000 (H) there is only one sharp peak. This would be interpreted as indicating no phase separation or the formation of a solid solution with a peak tan δ value at 294 K. Since in this polymer the hard and soft segments have approximately the same molecular weights, each is present to the extent of 50%. Using calculated glass transition temperatures of the hard segment of 380 K and of the soft segment of 214 K and the relationship

$$1/T_g = W_1/T_{g1} + W_2/T_{g2}$$

where W_1 and W_2 are the weight fractions of soft and hard segments, respectively, and T_{g1} and T_{g2} are the respective glass transition temperatures, the calculated T_g was 274 K, about 20 K lower than the experimental. This is attributed to the retention of the H-bonding of the hard segment when intimately mixed with the soft segment, an effect not accounted for in the complex equation for the glass transition temperature.

At and above 1000 molecular weight (I,J,K) two peaks in the tan δ curve are evident which are lower and farther apart as the molecular weight increases. The lower temperature peak is approaching that of the pure polyether and the upper

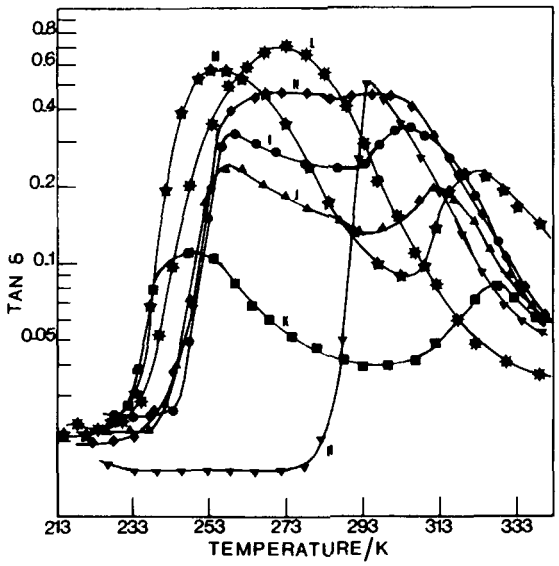

Fig. 3. Tan δ vs. temperature for polyurethanes based on ethylene glycol and MDI: with poly-(ethylene oxide) (mol wt): 600 (▼) (H); 1000 (●) (I); 1540 ;(▲) (J); 4000 (■) (K); with poly(propylene oxide) (mol wt); 1000 (✱) (L); 2000 (★) (M), and based on 1,5-pentanediol, MDI and poly(propylene oxide) mol wt 1000 (♦) (N). 110 Hz (see Table II for compositions).

temperature peak that of the pure urethane hard segment. For the polyether urethane based on poly(ethylene oxide) diol of molecular weight 1000 (I) the two peaks overlap considerably yielding a combined transition zone 65 K in width.

Similar data were obtained with poly(propylene oxide)diol (Fig. 3). When the molecular weight of the diol was 1000 (L) only one peak was observed with a maximum at 273 K, but, when the molecular weight was 2000 (M), two peaks were found, one at a lower and the other at a higher temperature than previously. It will be noted that the tan δ peaks are larger than the corresponding ones when poly(ethylene oxide)diol is used, presumably due to the more viscous nature of the polymer. However, the degree of phase separation seemed to be less, and there was some evidence of interphase structures or heterogeneities. Similar observations were made by Watts and White[15] using small-angle X-ray diffraction.

The data for the poly(ethylene oxide)diols for E' and E'' were calculated. For the polyether molecular weights of 1000 (I) and 1540 (J) the loss moduli are maximal between the two transition peaks. The value of the storage modulus is also high, and this coupled with the high values of tan δ suggests that energy dissipation would be great.

To further disrupt regularity in the polymer, poly(ethylene oxide)diol 1000 and 1,5-pentandiol (equal hydroxy equivalents) were reacted with MDI to yield a polymer (N) with irregular hard and soft segment lengths. The loss data are in Figure 3, and they show two overlapping peaks slightly higher than those for the corresponding poly(ethylene oxide)diol/ethylene glycol copolymer with regular hard segments. It is possible also that the pentandiol with the odd

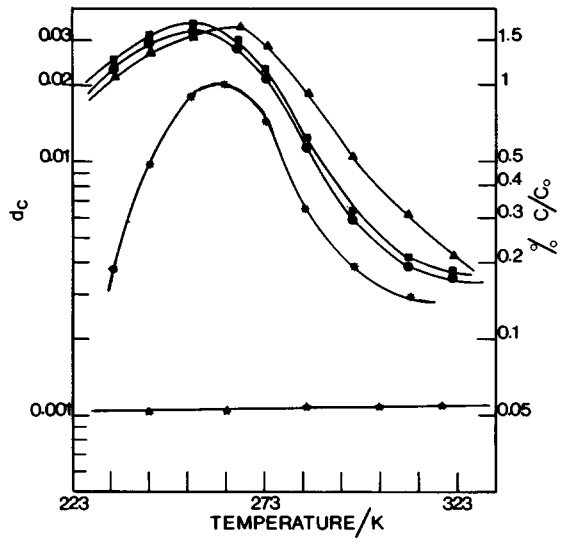

Fig. 4. Damping factor vs. temperature for polyurethanes based on Multrathane F242 and XB (D) on steel, $h_2 = 1$ at the 2nd mode (120–125 Hz) (■), 3rd mode (335–358 Hz) (●), and 4th mode (660–700 Hz) (▲), compared with uncoated steel at the 2nd mode (129 Hz) (★). Calculated from dynamic mechanical data (✱) (see Table I for compositions).

number of carbon atoms would not yield as much hard segment H-bonding just as crystallization in reduced with odd-numbered glycol units.[16]

The various copolymerization techniques possible with polyurethanes leads to quite wide ranges over which values of tan δ and the storage modulus are high, leading to high energy absorption and loss modulus over a wide temperature range. Bulky backbone ring groups in the flexible soft polymer, methyl side groups of the propylene units of the polyether soft segment, or disruption of the hard segment by an odd number methylene sequence are each effective.

Vibrational damping studies using these same polymers were undertaken in the extensional or free layer mode. The damping factors for the steel strips used were measured by the decay rate and varied over the first nine resonances from 14×10^{-4} for the first to 10^{-4} dB·s^{-1} for the 9th. For damping such vibrations in the extensional mode, Oberst[3] concluded that the loss modulus of the viscoelastic layer was the important factor, the other factors being constant.

The composite damping factor d_c for one of the viscoelastic materials on the steel strips is shown in Figure 4 for the polyester-bulky backbone ring diol polyurethane F242–XB (D). The second mode damping peaks occur at temperatures very close to the E'' maxima observed. The frequencies of the two tests are very close, 119 vs. 110 Hz. As the test frequency increased for the higher modes, the peak composite damping factor occurred at higher temperatures as would be expected. The data are expressed as percent critical damping factor also, the percent of the critical viscous damping coefficient which is the smallest value of damping for the system to undergo no oscillation. For comparison, most damping coatings have values of d_c between 0.02 and 0.3 and corresponding % C/C_0 from 1 to 15 over a temperature range of about 30 K. On this basis the materials tested have good damping properties between 233 and 273 K with

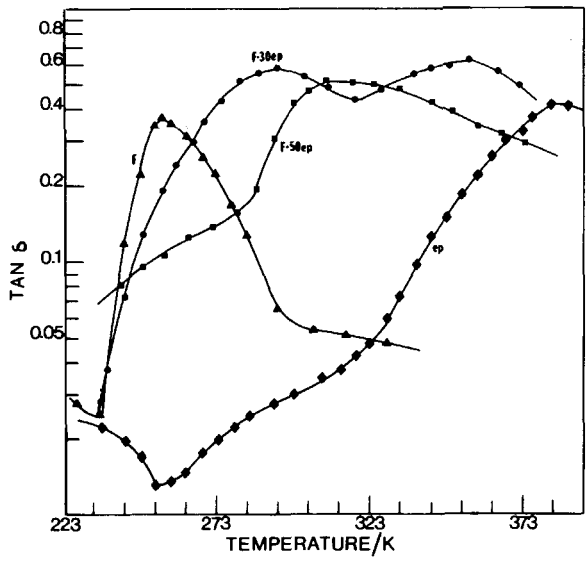

Fig. 5. Tan δ vs. temperature for polyurethane/epoxy blends: Multrathane F242/Multrathane R144 alone (▲) (F), epoxy alone (♦) (ep), 30% epoxy with polyurethane (●) (F–30 ep), and 50% epoxy with polyurethane (■) (F–50 ep); 110 Hz (see Table II for compositions).

better results being obtained when the bulky backbone ring diol was used. The efficiency of this viscoelastic material was not as much as anticipated from the tan δ curve alone because the storage modulus of the viscoelastic layer decreases rapidly with increasing temperature above T_g. The storage modulus of the steel–polyurethane composite decreased very slowly with increasing temperature. Using the dynamic mechanical data, the composite damping was calculated. The calculated values followed the experimental curve but were low.

Polyurethane–Epoxy Blends

Polyurethane–epoxy blends or pseudo-interpenetrating networks were prepared. The blended prepolymers and hardeners were allowed to react at 353 K to form the pseudo-interpenetrating network. It was assumed that there was no reaction between the two systems. The gel time for the polyurethane was about 6 min and that for the epoxy about 2 h. The two blends studied contained 30% (F–30 ep) and 50% (F–50 ep) epoxy. The data for tan δ, including those for the pure polymers, are in Figure 5.

The more continuous phase of the 30% epoxy sample (F–30 ep) appears to be polyurethane from the low modulus and also, as one would expect, from the larger amount and the shorter gel time.[17] The storage modulus indicates a complex morphological structure. When the epoxy is increased to 50% (F–50 ep) a plateau develops over the range 273 to 323 K suggestive of an intermediate phase or solid solution. The tan δ curves (Fig. 5) reinforce these views. The 30% epoxy sample (F–30 ep) shows two broad overlapping peaks at 290 and 365 K. The two peaks are, respectively, at higher and lower temperatures than for the pure polyurethane and pure epoxy polymers, and the peaks are higher and broader, indicating

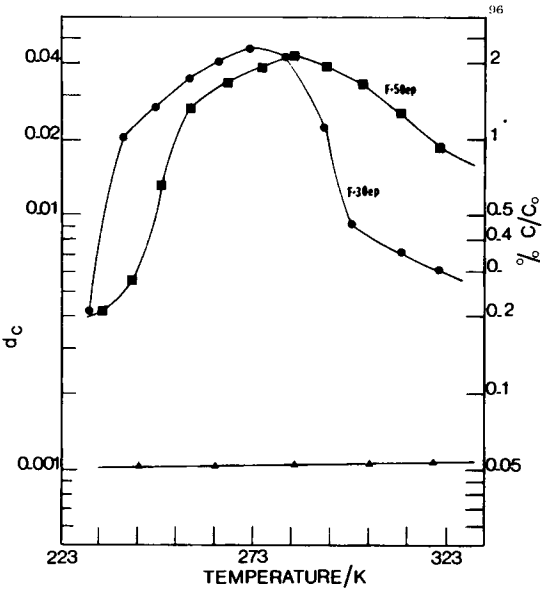

Fig. 6. Damping factor vs. temperature for polyurethane/epoxy blends of Figure 5. $h_2 = 1$: 30% epoxy (●) (F–30 ep) and 50% epoxy (■) (F–50 ep). Uncoated steel (▲). 2nd mode (120–125 Hz) (see Table II for compositions).

extensive interphase layers. When the epoxy content is increased to 50% (F–50 ep) there is just one very broad tan δ peak with high values over a wide temperature range from 273 to at least 363 K. The structure is quite heterogeneous. Since the loss modulus E'' is the product of E' and tan δ, one would expect excellent damping when this blend is used, particularly the 30/70 epoxy/polyurethane mixture (F–30 ep). Similar observations were made with acrylic polymer[18] and vinyl polymer[5] blends.

The composite damping factor when the epoxy–polyurethane viscoelastic layer was used are in Figure 6. Incorporation of 30% epoxy (F–30 ep) shifted the peak from 245 to 273 K, and the values are higher due to the higher storage modulus of the blend. When the blend contains 50% epoxy (F–50 ep), the composite damping factor is higher over the temperature range 283–313 K. A substantial improvement over the data in Figure 4 can be noted.

The opportunity was taken to check the effect of thickness with the last mentioned blend, F–50 ep. A plot of the ratio of the composite damping factor to the damping factor for the viscoelastic layer was made for the polyurethane based on F242 and R144 (F) and a 50:50 blend of this with epoxy (F–50 ep). In neither case, although the ratio increased rapidly with thickness, was a saturation value reached with thickness ratios of 5 or 6.

Effect of Fillers in Polyurethane

Fillers have the same effect as hard segments providing there is adequate adhesion between the phases. Fillers often increase the dynamic and loss moduli and the loss factor yielding an apparently higher glass transition temperature for the matrix. Figure 7 shows the data for the tan δ when mica is added to the

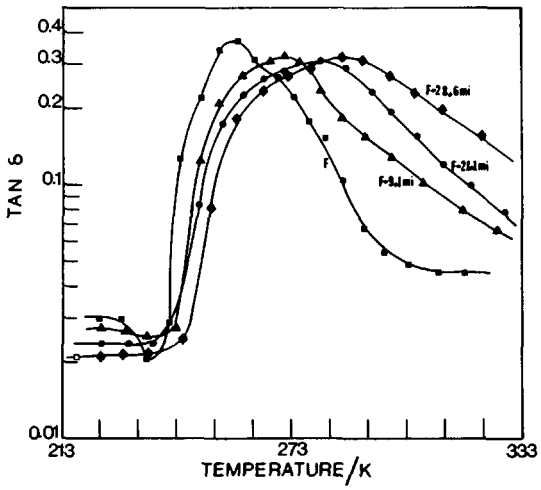

Fig. 7. Tan δ for mica filled polyurethane, Multrathane F242/Multrathane R144 alone (■) (F), 9.1 vol % mica (▲) (F–9.1 mi), 21.1 vol % mica (●) (F–21.2 mi), and 28.6 vol % mica (♦) (F–28.6 mi). 110 Hz (see Table II for compositions).

polyurethane matrix (F). The addition of mica increases the storage moduli greatly and shifts the loss peaks to higher temperatures, from 258 to 281 K, with significant broadening on the high temperature side of the peak. This is attributed[19–21] to adhesion of the polymer to filler so that the segmental relaxation times are increased (and also to the enhanced strain imposed on the polymer between the filler particles, leading to shorter relaxation times).

The maximal values of tan δ as a function of volume fraction of filler were slightly lower when −325 mesh calcium carbonate was used when compared with −10 + 20 mesh mica, over the range studied, and up to 0.3 volume fraction. The values were almost constant between 0.1 and 0.3 volume fraction, i.e., the major effect was observed below 0.1 volume fraction. However, the peaks when higher volume fractions were used were broader particularly towards the high temperature side of the peak.

In Figure 7 it will be noted that increasing volume fraction of filler resulted in a lower tan δ below the peak, i.e., in the glassy region. This same effect was observed with −10 + 20 mica in polypropylene to the extent of 0.14, 0.23, and 0.31 volume fractions. The damping d_c of the blend decreased from 0.037 for the pure polypropylene to 0.033, 0.026, and 0.021, respectively. These values were close to those calculated[22] from the equation

$$\tan \delta = \tan \delta_m \, V_m$$

in which tan δ_m is the loss factor for polypropylene and V_m is the volume fraction of polypropylene. The calculated values were 0.032, 0.023, and 0.026, respectively, measured at the second resonance mode. Similar data were obtained at the third resonance mode. An earlier study[14] showed that, as the particle size of mica is decreased, the tan δ peak occurs at slightly higher temperatures but the height is not affected. The particle size of calcium carbonate appeared to have less effect, −325 mesh raised the peak to 296 K for a thermoplastic polyurethane, Texin 355D, whereas the changes were to 294, 297, and 300 K respec-

TABLE II
Properties of Various Systems

Sample code	Composition designation	Temp range (K) (tan $\delta > 0.15$)	tan δ_{max}	E' range (Pa) (transition zone)	$T_{max\ E''}$ (K)
F	F242–R144	246–281	0.365	9×10^7–1.4×10^9	239
E	F242–F222	243–273	0.36	8.7×10^7–1.5×10^9	235
C	F242–XA	257–308	0.44	9.5×10^7–1.6×10^9	252
D	F242–XB[a]	259–	0.48	9.5×10^7–1.6×10^9	257
A	F242–1,4-butanediol	254–287	0.42	1×10^8–1.9×10^9	246
B	F242–1,10-decanediol	250–298	0.56	9×10^7–1.45×10^9	241
G	F242–1,4-cyclohexanediol[a]	253–	0.48	9×10^7–1.6×10^9	251
C/F-75/25	F242–75XA–25R144[b]	253–285	0.42	9×10^7–1.5×10^9	247
C/F-50/50	F242–50XA–50R144[b]	249–294	0.41	9×10^7–1.5×10^9	247
C/F-25/75	F242–25XA–75R144[b]	245–291	0.49	9×10^7–1.5×10^9	244
D/F-75/25	F242–75XB–25R144[b]	251–295	0.49	9×10^7–1.5×10^9	253
D/F-50/50	F242–50XB–50R144[b]	248–295	0.47	9×10^7–1.5×10^9	251
D/F-25/75	F242–25XB–75R144[b]	248–291	0.40	9×10^7–1.5×10^9	251
H	PE0600–MDI–ethylene glycol	291–316	0.50	9×10^7–1×10^9	285
I	PE01000–MDI–ethylene glycol	253–319	0.35	1.9×10^8–1×10^9	262
J	PE01540–MDI–ethylene glycol	252–318	0.26	1.9×10^8–1×10^9	256
K	PE04000–MDI–ethylene glycol[c]	237–267, 317–341	0.12	1.2×10^8–1.1×10^9	253
L	PP01000–MDI–ethylene glycol	247–298	0.63	1×10^8–2×10^9	255
M	PP02000–MDI–ethylene glycol	241–287, 313–337	0.60	1×10^8–1.7×10^9	238
N	PE01000–MDI–pentanediol	252–319	0.46	1×10^8–1×10^9	259
F–30 ep	F242–R144–30% epoxy[a]	251–	0.6	1.5×10^8–2.8×10^9	256
F–50 ep	F242–R144–50% epoxy[a]	281–	0.52	2×10^8–3×10^9	291
F–9.1 mi	F242–R144–9.1 vol % mica	251–293	0.32	1.8×10^8–2×10^9	255
F–21.1 mi	F242–R144–21.1 vol % mica	253–305	0.31	3×10^8–3×10^9	258
F–28.6 mi	F242–R144–28.6 vol % mica	257–318	0.32	9×10^8–5.8×10^9	263
F–9.6 cc	F242–R144–9.6 vol % $CaCO_3$	253–298	0.30	2×10^8–2×10^9	256
F–26.9 cc	F242–R144–26.9 vol % $CaCO_3$	255–306	0.31	2×10^8–3×10^9	258

[a] No upper limit temperature can be obtained.
[b] Numbers refer to % hydroxyl equivalent.
[c] Transition range based on tan $\delta > 0.06$.

tively for −40 + 70, −80 + 325, and −325 mesh mica. This agrees with the concept of greater adsorption on the larger surface areas of the smaller particles which takes place with mica but not to the same extent with calcium carbonate.

In general, reactive fillers broaden the loss peaks on the high side and move the peak to higher temperature and thus would be expected to improve the damping performance.

The increase in damping with volume loading is limited to a range up to perhaps 0.4 volume fraction. It has been observed[23] that above 0.45 volume fraction the values of tan δ decrease.

Since the damping factor is the product of the loss factor and dynamic modulus, the temperature range over which tan δ is greater than 0.15, the values of E' over the range where tan δ exceeds 0.06, the temperature at which E'' is a maximum, and the maximal value of tan δ observed are tabulated in Table II for comparison of effectiveness.

Based on time–temperature superposition principles, a change of frequency by one decade is equivalent to a temperature shift of 7 K. Thus the above data show that the various compositions would be effective over many decades of frequency above and below the test frequency of 110 Hz at the temperature of the maximal damping. Of course, as the operating temperature moves towards either of the extremes, the utility of the viscoelastic materials diminishes in the "short" direction of the scale.

Most of the curves of data were complex, and there seemed to be little hope of obtaining meaningful master curves. Some of the data were so treated, and the results are in Table III. These were obtained by manually shifting the dynamic modulus data with respect to a reference frequency and temperature. The shift factor with respect to temperature was calculated. Plotting the difference between the temperature and the reference temperature vs. the ratio of this difference to the log of the shift factor to base 10 yielded lines, the straight portions of which yielded a slope of $-1/C_1$ and an intercept of C_2, according to the WLF equation

$$\log_{10} a_T = - C_1(T - T_0)/[C_2 + (T - T_0)]$$

No particular significance is attributed to the numerical values of C_1 and C_2. However, they lie in the ranges of values obtained for pure polymers and for filled

TABLE III
T_g and WLF Constants

Sample code	Polymer system	WLF constants C_1	WLF constants C_2 (K)	T_0 (K)	Glass transition temperature T_g (K)
F	F242–R144	2.85	25.05	253	224
C	F242–XA	6.27	30.46	273	249
D	F242–XB	5.32	54.1	273	252
A	F241–1,4-butanediol	3.76	14.2	269	240
B	F242–1,10-decanediol	3.38	12.8	268	235
G	F242–1,4-cyclohexanediol	5.12	51.9	273	247
F–21.2 mi	F242–R144–21.1 vol % mica	18.74	101.5	280	—
F–28.6 mi	DF242–R144–28.6 vol % mica	11.84	162.1	281	—
ep	Epoxy (Epon 815)	–	—	—	385

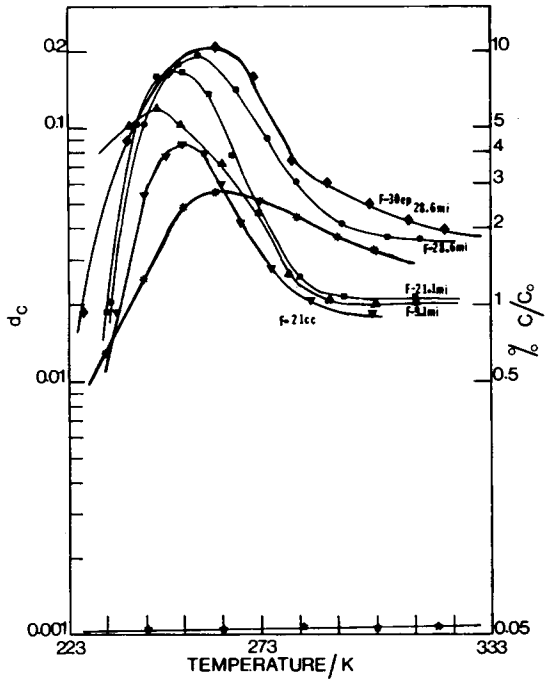

Fig. 8. Damping factor of filled polyurethanes based on Multrathane F242/Multrathane R144 (F) and fillers: 2nd mode resonance 110–160 Hz, h_2 = 1.5 for 9.1 vol % mica (▲) (F–9.1 mi), 21.1 vol % mica (■) (F–21.1 mi), and 28.6 vol % mica (●) (F–28.6 mi) and calculated for 28.6 vol % mica (∗): 2nd mode resonance 115–117 Hz, h_2 = 2.2 for 30% epoxy blend (F–30 ep) with 28.6 vol % mica on total polymer (♦) and 2nd mode resonance 100–170 Hz, h_2 = 1.5 for blend of (F) with 21 vol % calcium carbonate (▼) (F–21 cc). Uncoated steel (★) 2nd mode (120–125 Hz) (see Table II for compositions).

systems, and may be used to predict performance of individual polymers under conditions other than those attained in the experiments. Note that the data refer to the lower temperature peaks of the soft segment, not the higher temperature hard segment. The reference temperatures were 20–35 K above the T_g as measured by differential scanning calorimetry.

Fillers broaden the loss peaks and raise the storage modulus both of which are favorable for increased damping of composites. The effect of −10 + 20 mesh mica (planar filler) on the composite damping of the polyurethane (F242–R144) (F) is shown in Figure 8. As the mica content increases, the damping is increased and the peak broadened in the higher temperature direction. Indeed the damping remains high above the glass transition temperature. Specifically when 28.6 vol % of mica (F–28.6 mi) is used, the storage modulus decreases only from 7 to 1 GPa between 233 and 313 K, an order of magnitude higher than for the matrix alone, which decreases from about 2 to 0.07 GPa over this range.

The tan δ values of the filled polymer do not differ as much being in fact somewhat lower below 263 K and somewhat higher above 283 K than for the matrix. Nevertheless, the product as expressed by E'' is substantially higher. Ball and Salyer[5] also observed that planar fillers were effective in extensional damping.

The effect of frequency is not marked. When 21.1 vol % mica is used (F–21.1 mi), the composite damping peaks shift towards higher temperatures at the higher response frequencies. The effect of thickness was as before. As the thickness ratio increases the ratio of the composite damping to the damping of the viscoelastic layer is increased. With 28.6 vol % mica (F–28.6 mi), saturation appeared to be reached at a thickness ratio of about 2.8. When 21.1 vol % (F–21.1 mi) was used, saturation was not reached but appeared to be occurring at a much lower thickness ratio than for the matrix itself. On a log–log plot, the ratio of the composite damping to matrix damping obeyed a 3.5 and 3 power relationship with the thickness ratio. This higher power was predicted by Oberst[3] and Ungar[7] for regions of high damping.

The effect of fillers on the already good damping properties of the epoxy–polyurethane blend 30/70 (F–30 ep) is shown in Figure 8. The composite damping factor follows a curve similar to that for the pure polyurethane matrix (F). Maximal damping occurs at 263 K, a temperature close to the temperature of the E'' peak. Above 293 K the damping remains relatively constant and high. The second relaxation was observed in this range in the dynamic mechanical tests. Although the tan δ values of the two transitions were approximately the same, the lower storage modulus of the blend over the temperature range of the second peak results in a lower composite damping factor.

The effect of calcium carbonate when used as a filler in a polyurethane matrix was very similar. The dynamic mechanical properties are in Figure 1 for the matrix alone (F). With 21 vol % of filler (F–21cc) for the damping results (Fig. 8) were similar to but lower than those obtained with mica filled samples.

The composite damping factor is directly proportional to the E'' of the matrix so that the composite damping factor can be calculated from the loss moduli. This was done for the polyurethane F242–R144 with 28.6 vol % mica (50 wt %) (F–28.6 mi) (Fig. 8). The shape of the curve is similar to the experimental, but the calculated data are lower, and the deviations are greater at the lower temperatures. Therefore, qualitatively the theories of Oberst[3] and Ungar[7] predict the composite damping factor in the extensional mode.

Constrained Layer Damping

In this study the steel base plate was coated with the viscoelastic layer and then a layer of aluminum foil (0.1 or 0.2 mm) or epoxy resin was added as the constraining layer. The moduli of the steel, aluminum, and epoxy were, respectively, 2×10^{11}, 7×10^{10}, and $1.5–3.0 \times 10^{9}$ Pa.

When the polyurethane F242–R144 (F) and aluminum foil was used, the data shown in Figure 9 were obtained. The composite damping factor curves are very similar to the corresponding tan δ curve (Fig. 1) except that the peak of the former is shifted to higher temperatures, in part due to the higher frequency and in part due to the metal polymer interface where some polymer is immobilized. Similar data were obtained with a polyurethane based on poly(ethylene oxide) diol of 1000 molecular weight and a hard segment composed of MDI and ethylene glycol (I). The composite damping factors are in Figure 9. The curve is very similar to the tan δ curve (Fig. 3), where the peaks were at 260 and 305 K. These data illustrate well Kerwin's[6] theory that the composite damping factor depended on the loss factor of the viscoelastic layer. The tan δ of the polyurethane F242–R144 (F) is lower than that for the polyether polyurethane (I) above 273

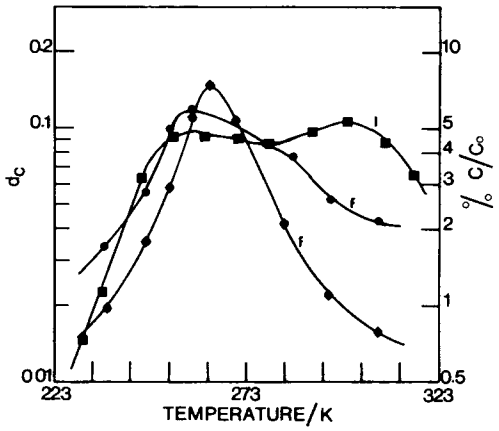

Fig. 9. Constrained layer damping, steel and aluminum with Multrathane F242/Multrathane R144 (F), $h_2 = 1$, $h_3 = 0.32$ at the 2nd mode (♦) and at the third mode (●) (672–900 Hz), with ethylene glycol/MDI/poly(ethylene oxide) mol wt 1000, $h_2 = 0.8$, $h_3 = 0.32$, 2nd mode resonance 250–350 Hz (■) (I) (see Table II for compositions).

K and the damping is less. The difference below 273 is less obvious since the ratio H_2/H_1 (h_2) is larger, which would raise the damping slightly. As would be expected, the composite damping of the constrained layer mode increased with h_2.

For the constrained layer system two parameters, a geometric parameter X and a shear parameter Y may be defined. Under otherwise identical conditions, Y depends only on H_2. X may be calculated for various values of H_2 knowing the moduli of the steel and aluminum and estimated shear modulus from the storage moduli obtained from dynamic mechanical tests, ignoring the differences in test frequencies. Plots of X and Y vs. H_2 were linear. Also knowing X and Y enabled one to calculate the composite damping factor as a function of H_2. When compared with actual values, obtained when the damping and the shear modulus G' of the damping layer were, respectively, 0.36 and 1.86×10^8 Pa, the experimental data were higher but followed the same curve over the range $h_2 = 0.6$–1.0.

When all other factors are constant, the modulus and the thickness of the constraining layer has an effect. This was determined for the epoxy–F242–R144 blend (F–30 ep). Doubling the thickness of the aluminum foil resulted in higher damping. The lower modulus epoxy constraining layer, even at greater thickness, was less effective. The storage modulus for such constrained layer systems decreased slowly with increasing temperature.

The effect of resonance frequency on the results using a random copolymer of F242–R144–XA (ratio of XA to R144 75/25 equivalents) (C/F-75/25) is shown in Figure 10. The composite damping factor behaves as predicted, the peak occurs at higher temperatures with higher frequencies.

General Discussion

The composite damping factor in extensional mode depends on the loss modulus, i.e., the product of the dynamic modulus and the loss factor of the viscoelastic layer. Thus optimal damping occurs at a temperature about 20 K

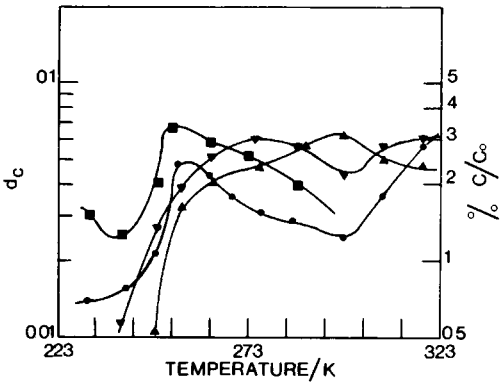

Fig. 10. Constrained layer damping factor for steel and aluminum with Multrathane F242/Multrathane R144–XA (C/F-75/25), $h_2 = 0.8$, $h_3 = 0.32$, at the lst mode (21–27 Hz) (■), 2nd mode (138–190 Hz) (●), 3rd mode (358–550 Hz) (▼), and 4th mode (650–1103 Hz) (▲) (see Table II for compositions.)

below the glass transition temperature where the modulus is still high. When fillers are included, the loss factor also remains high and higher than predicted, particularly for planar mica filler which adds significantly to the flexural modulus and results in higher moduli above the glass transition temperature. It was worth calculating the effect of the mica on the basis of the filler being in a layer and acting as a constraining layer. When 0.286 volume fraction of mica is used, $E = 7.1 \times 10^{10}$ Pa, in a viscoelastic layer 1.5 times the thickness of the steel, the second mode complex damping factor could be calculated for various temperatures using the tan δ values for the polyurethane R242–R141 (F). The data are in Table IV and show clearly that the experimental results calculated on the assumption of a constrained system are close to a similar constrained system using aluminum foil. As mentioned earlier, the calculated values for the extensional mode are lower than the experimental, particularly at the lower temperatures.

For the constrained layer configuration the tan δ of the viscoelastic layer is important whereas the storage modulus is not but rather the bending stiffness of the constraining layer. Obviously the variation of E' and tan δ of the viscoelastic layer with temperature is important. The E' of the composite is likewise important in applications. The values for steel and typical composite were calculated. The modulus approximates that for steel multiplied by its volume fraction in the composite. Likewise the modulus remains fairly constant with

TABLE IV
Comparison of d_c Values for 28.6 Vol % Mica-Filled F242–R144 (F–28.6 mi) with Aluminum Constrained F242–R144 (F)

Temp (K)	28.6 vol % mica-filled F242–R144 (F–28.6 mi)			Al-constrained F242–R144 (F)
	d_c exptl	d_c calcd extensional	d_c calcd constrained	d_c exptl
253	0.18	0.044	0.08	0.06
273	0.19	0.086	0.054	0.09
293	0.04	0.059	0.014	0.02
313	0.034	0.022	0.01	0.015

TABLE V
Damping Properties of Polyurethane Systems

Sample code	Viscoelastic layer	Coating configuration	Thickness ratio h_2	Temp range (K)	d_c range
F	F242–R144	Extensional	1	233–293	0.004–0.028
C	F242–XA	Extensional	1	243–293	0.005–0.03
D	F242–XB	Extensional	1	233–300	0.004–0.035
F–30 ep	F242–R144–epoxy 30%	Extensional	1	233–300	0.006–0.044
F–50 ep	F242–R144–epoxy 50%	Extensional	1	240–330	0.006–0.043
I	PE01000–MDI–ethylene glycol	Extensional	1	240–310	0.006–0.04
F–9.1 mi	F242–R144–9.1 vol % mica	Extensional	1.5	233–320	0.02–0.12
F–21.1 mi	F242–R144–21.1 vol % mica	Extensional	1.5	230–320	0.02–0.18
F–28.6 mi	F242–R144–28.6 vol % mica	Extensional	1.5	230–320	0.02–0.20
F–30 ep 28.6 mi	F242–R144–epoxy (70/30)–28.6 mica	Extensional	2.2	230–320	0.02–0.22
F–21 cc	F242–R144–21 vol % $CaCO_3$	Extensional	1.5	233–293	0.02–0.085
I–21 cc	PE01000–MDI–ethylene glycol–21 vol % $CaCO_3$	Extensional	2.5	233–323	0.02–0.11
F	F242–R144	Constrained	1	230–310	0.02–0.13
C	F242–XA	Constrained	1	230–310	0.02–0.15
D	F242–XB	Constrained	1	230–310	0.03–0.15
I	PE01000–MDI–ethylene glycol	Constrained	0.8	230–320	0.02–0.10
F–30 ep	F242–R144–epoxy 30%	Constrained	1.2	273–330	0.02–0.16
F–50 ep	F242–R144–epoxy 50%	Constrained	1	273–330	0.02–0.15
F–30 ep[a]	F242–R144–epoxy 30%[a]	Constrained	1.2	283–330	0.02–0.058
F–30 ep[b]	F242–R144–epoxy 30%[b]	Constrained	1.2	283–330	0.02–0.06

Note. Constraining layer is aluminum, $h_3 = 0.32$.

[a] $h_3 = 0.16$, aluminum layer.

[b] Constraining layer is epoxy, $h_3 = 0.6$.

frequency, the decrease with increasing frequency being slightly more the higher the frequency. A summary of the data is in Table V.

SUMMARY

Polyurethanes based on polyester and polyether prepolymers have fairly large loss factors or good damping properties in the region of the glassy transition temperatures, which are distinct when the two phases tend to separate and merge when the two phases are compatible. The damping properties may be increased by using bulky backbone or methyl branched monomer units such as a tricyclodecanediol or a diol based on propylene oxide, respectively, rather than ethylene oxide.

The width of the loss peak and its location varied with the ratio of epoxy to polyurethane in a pseudo-interpenetrating network structure. With 50% by weight of epoxy (F–50 ep) the two peaks overlapped leading to a single very broad damping range. With 30% by weight of epoxy (F–30 ep) there were two peaks, farther apart. The incorporation of mica or calcium carbonate shifted the peaks of the polyurethane damping to higher temperatures and raised the loss factor. A particularly effective combination was mica-filled polyurethane–epoxy blend.

The damping properties measured on the Rheovibron at 110 Hz were compared with those obtained at the resonance frequencies of steel panels (or strips) coated with the same polymer and measured on the Brüel and Kjaer Damping Modulus Apparatus. There was a qualitative similarity in the results both when an extensional mode was used with a single layer of polyurethane and when a constrained layer configuration was used with the polyurethane between the steel and a constraining layer of aluminum or epoxy.

In the extensional mode, it was confirmed that the damping is related to the loss modulus of the viscoelastic layer and was greater the higher the storage modulus. In the constrained layer configuration the damping was also better the higher the storage modulus and was related to the loss factor of the viscoelastic layer.

Mica, lying in the plane of the polyurethane layer, could be considered as a constraining layer since on calculating the vibration damping effectiveness from the loss factor, the data calculated for the constrained configuration more closely approximated the actual data than did the values calculated for the extensional mode. Calculated values of the vibration damping tended to be lower than the experimental values. However, Rheovibron data can be used to predict the shape of the vibration damping curves and the approximate values.

Polyurethane compositions capable of damping vibrations over a very wide temperature range, and also frequency range, can be made easily.

The University of Toronto and the National Research Council of Canada are thanked for a scholarship and fellowship respectively for DTHW. Supported by the National Research Council of Canada, the Natural Sciences and Engineering Research Council of Canada, and Polysar Ltd. Presented in part at the Canadian Society for Chemical Engineering Conference, Toronto, October 1976, the SPE ANTEC Conference, Boston, May 1981, and the IUPAC International Symposium on Macromolecules, Strasbourg, July 1981.

References

1. J. P. Den Hartog, *Mechanical Vibrations*, McGraw-Hill, New York, 1934.
2. C. Zwikker and C. W. Kosten, *Sound Absorbing Materials*, Elsevier, New York, 1949.
3. H. Oberst, *Acustica*, *Akust. Beih.*, **2**(4), 181 (1952); H. Oberst, L. Bohn, and F. Linhardt, *Kunstoffe*, **51**, 495 (1961).
4. D. Ross, E. E. Ungar, and E. M. Kerwin, Jr., *Structural Damping*, J. E. Ruzika, Ed., ASME, New York, 1959, p. 49.
5. G. L. Ball III and I. O. Salyer, *J. Acoust. Soc. Am.*, **39**, 663 (1966).
6. E. M. Kerwin, Jr., *J. Acoust. Soc. Am.*, **31**, 952 (1959).
7. E. E. Ungar, *Noise and Vibration Control*, L. L. Beranek, Ed., McGraw-Hill, New York, 1971, Chap. 14.
8. T. P. Yin, T. J. Kelly, and J. E. Barry, *J. Eng. Ind. (Trans. ASME)*, **89**, 773 (1967).
9. D. M. Preiss, W. C. Rodgers, and D. W. Skinner, *Rubber Age*, **2**, 61 (1967).
10. A. F. Lewis and G. B. Elder, *Adhesive Age*, **12**(10), 31 (1969).
11. T. P. Yin, *Sci. Am.*, **220**(1), 98 (1969).
12. A. C. F. Chen and H. Leverne Williams, *J. Appl. Polym. Sci.*, **20**, 3387 (1976).
13. A. C. F. Chen and H. Leverne Williams, *J. Appl. Polym. Sci.*, **20**, 3403 (1976).
14. D. T. H. Wong, M.A.Sc. Thesis, University of Toronto, 1975.
15. M. P. C. Watts and E. F. T. White, *Polym. Prepr., Am. Chem. Soc.*, **19**(1) 38 (1978).
16. H. Yip and H. Leverne Williams, *J. Appl. Polym. Sci.*, **20**, 1209, 1217 (1976).
17. R. E. Touhsant, D. A. Thomas, and L. H. Sperling, *J. Polym. Sci., Polym. Symp.*, **46**, 175 (1974).
18. J. A. Grates, D. A. Thomas, E. C. Hickey, and L. H. Sperling, *J. Appl. Polym. Sci.*, **19**, 1731 (1975).
19. R. F. Landel, *Trans. Soc. Rheol.*, **2**, 53 (1958).
20. Yu. S. Lipatov, V. F. Babich, and V. F. Rosovizky, *J. Appl. Polym. Sci.*, **20**, 1787 (1976).
21. K. Lisak and K. Shibayama, *J. Appl. Polym. Sci.*, **22**, 1845 (1978).
22. L. E. Nielsen, *Mechanical Properties of Polymers and Composites*, Marcel Dekker, New York, 1974, Vol. 2.
23. W. H. Brueggemann and P. J. DeFranco, *32nd Annual Tech Conf. SPE*, 314 (1974).

Received October 12, 1982
Accepted January 21, 1983